An ITC and NMR Study of Interaction and Complexation of Asphaltene Model Compounds in Apolar Solvent I: Self-Association Pattern

Sébastien Simon, Duo Wei*,**, Mathilde Barriet, Johan Sjöblom*

Ugelstad Laboratory, Department of Chemical Engineering, the Norwegian University of Science and Technology (NTNU), N-7491 Trondheim, Norway

KEYWORDS. Self-association, precipitation, solubility, interaction, asphaltene model compounds.

ABSTRACT. The self-association pattern of asphaltene model compounds with different functional groups in xylene and mixtures of xylene and heptane have been studied by isothermal titration calorimetry (ITC) to shed new light on the association and interaction between components in the asphaltene fraction. The model compounds are N-(1-undecyldodecyl)-N'-(5-carboxylicpentyl)perylene-3,4,9,10-tetracarboxylbisimide (C5PeC11) and N,N'-bis(1-undecyldodecyl)perylene-3,4,9,10-tetracarboxylbisimide (BisAC11).

The results show that a combination of hydrogen bonding due to carboxylic groups and π-π stacking due to polyaromatic rings leads to higher association extent of C5PeC11 compared to that of BisAC11 in xylene. A dimerization model can well fit the association of both model compounds in xylene obtained both by ITC and NMR. Mixtures of C5PeC11 and BisAC11 can well quantitatively fit the features of self-association of real extracted asphaltenes probed by ITC. This could mean that the total asphaltene fractions are composed of polydisperse compounds displaying very different association properties.

Finally, increasing the heptane content in the solvent results in higher extent of π-π stacking between C5PeC11 molecules, which indicate formation of larger aggregates or tighter arrangement of aromatic rings.

1. INTRODUCTION

Asphaltenes are a fraction of petroleum crude oil and responsible for numerous problem during oil production, separation and transportation.[1-4] They can stabilize water-in-oil emulsions[5, 6] impacting oil-water separation. They can also precipitate and form organic deposits in reservoirs, wells, piping and equipment by change of pressure[7-9] or mixing with incompatible fluids.[10, 11] This can lead to costly well-fluid flow restrictions and unplanned production irregularities and shut-ins.

Asphaltenes are insoluble in n-alkanes but soluble in aromatic solvents like toluene or xylene. They constitute thousands of molecules with different molecular weights and functionalities. The typical mean molecular weight of asphaltenes is ca. 750 g/mol with a factor of 2 in the width of the molecular weight distribution.[12-18] Two main models have been proposed to describe a typical asphaltene molecule: the archipelago model in which asphaltenes are thought to consist of small polyaromatic parts linked together by aliphatic or naphthenic moieties, and the continental model considering asphaltene molecules constituted of single polyaromatic ring with side-linked aliphatic or naphthenic chains.[19, 20] In both models heteroatoms occur in a variety of cyclic and aliphatic locations. Asphaltenes are both basic and acidic, the latter due to the presence of carboxylic acid functions most likely in the alkyl-side chains[21, 22].

The asphaltenes are prone to self-associate in model hydrocarbon solvents or petroleum crude oils. Two different scales and phenomena need to be differentiated.

-First, the nanometer scale. In toluene or in correspondingly “good” enough solvent, asphaltenes self-associate to form nanometer-sized aggregates. The terms of nanoaggregates and clusters are sometimes used to describe more accurately the formed aggregates.[20] These aggregates seem to be stable.

-Second, the micrometer scale indicating asphaltene precipitation. If the precipitation is induced by adding a non-solvent like an alkane, then asphaltenes precipitate by flocculating until forming micrometer-sized flocs. The kinetics of formation of these flocs follows classical colloid flocculation kinetics like the diffusion and reaction-limited aggregation.[23, 24]

The wide distribution of molecular weight as well as the hydrocarbon complexity and heteroatom heterogeneity results in an enormous challenge in terms of description of asphaltene system from molecular levels. To solve this problem,[4] one experimental approach is to fractionate asphaltenes into several sub-fractions by changing the ratio of good solvent/precipitate solvent,[25-28] ultracentrifugation,[29, 30] or ultrafiltration.[31, 32] However, even after the fractionation, the asphaltene fractions still contain a large number of compounds with a wide distributions of molecular weight and structures. In order to overcome

this structural problem, several groups[4, 33-36] have focused on the design of asphaltene model compounds which have high purity and well-defined molecular structure.

Sjöblom and his group have designed a family of asphaltene model molecules composed of a perylene polyaromatic core linked to a fixed hydrophobic part and a variable group, polar or apolar.[35, 37, 38] This structure is consistent with the continental model mentioned above even if the model molecules contain more oxygen than asphaltenes. They found that the interfacial and emulsion stabilization properties of these molecules depend strongly on the structure suggesting that a small fraction of asphaltenes could be responsible for crude oil emulsion problems.[39]

For asphaltene association Mullins proposed the Yen-Mullins model claiming that the major driving force is π-π stacking. This interaction leads to asphaltene nanoaggregates with an aggregation number[20] less than 10. Gray et al.[40] proposed a supermolecular assembly model of asphaltenes, combining cooperative binding by acid-base interactions, hydrogen bonding, metal coordination complexes, and interactions between cycloalkyl and alkyl groups to form hydrophobic pockets, in addition to aromatic π-π stacking leads to strongly associated structure of asphaltenes, although all the forces taken individually are very weak. Sedghi et al.[41] studied the self-association of asphaltenes by molecular dynamics (MD). They found that interactions between aromatic cores are the major driving force for association as the energy of association

increases substantially with the number of aromatic rings. Heteroatoms also influence asphaltene self-association as well as their location either in the aromatic cores or attached to the aliphatic chains. Aliphatic chains attached to the aromatic core limit aggregation by steric repulsion, also addressed by MD calculations by Jian et al.[42] In conclusion, the level of the asphaltene aggregation will depend on the size of aromatic rings, and the amount and state of heteroatoms such as N, O, and to a lesser extent S and aliphatic chains.[33, 34, 43] However, there are only a few experimental evidences to confirm these predictions.

In this paper, the first of a series of two, the self-association properties of model compounds containing different functionalities were determined. These model compounds represent the asphaltenes of the continental type, and aims to mimic only parts of the total asphaltene fraction: either acidic (C5PeC11) or non-acidic (BisAC11) (Figure 1).[44] The aim is to differentiate effects from the different types of molecular interactions. The interplay and complexation between model compounds and between model compounds and asphaltene precipitation inhibitors will be studied in the second part of the series.

2. MATERIALS AND METHODS

All chemicals were used without purification and were purchased from VWR. Xylene was a mixture of isomers and had a purity of 99.2%. The asphaltene model compounds C5PeC11 and BisAC11 were synthesized according to previously reported procedures.[37, 45] Structures and

molecular weight of the model compounds are presented in Figure 1. The maximum solubility of C5PeC11 in xylene was determined to be 3.0 g/L (3.8 mM) at room temperature. Below this concentration, the C5PeC11 solutions were found stable with no variations in their UV spectra within two weeks.

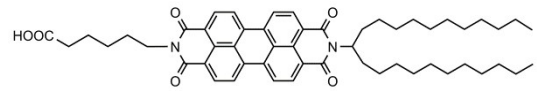

C5PeC11 M_W=827.11 g/mol

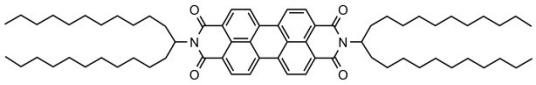

BisAC11 M_W=1035.61 g/mol

Figure 1. Chemical structure of C5PeC11 and BisAC11

2.1 Isothermal titration calorimetry (ITC)

NANO-ITC Standard volume from TA instruments was used to perform isothermal titrations. The procedure of the experiments has been well documented in our previous article.[46] All tests were carried out at 25 ºC with the stirring rate of 250 rpm. The injection interval was 400 s to let system equilibrate. A blank experiment with xylene titrated into xylene accounting for friction heat was subtracted from the experimental data before any further analysis. NanoAnalyze™ (TA Instruments) was applied to analyze and fit the ITC data. Solutions of asphaltene model compounds were prepared by dissolving the solid compounds in xylene and then sonication for

30 min. The solutions were kept in the dark overnight prior to each measurement to ensure homogeneity. All solutions were re-sonicated for 30 min right before measurements to ensure that no bubbles were present. All the experiments have been repeated at least twice.

2.2 Nuclear magnetic resonance (NMR)

^{1}H NMR measurements were carried out on a BrukerAdvance DPX spectrometer operating at 400 MHz. The model compounds were dissolved in d-toluene and sonicated for 30 min. The number of scans for 0.1 g/L C5PeC11 was 512, and, for all other samples was, 256.

2.3 UV-visible spectroscopy

UV-240PC (Shimadzu) was used to obtain the UV-visible spectra. A 2 mm cell was used. The wavelength range was from 700 nm to 240 nm with the interval of 1 nm. Scanning speed was slow and slit width was 2.0 nm. To eliminate background effects, the reference cuvette was filled with the same mixture of xylene/heptane.

3. RESULTS AND DISCUSSION

3.1 Self-association of asphaltene model compounds

3.1.1 Self-association of C5PeC11

In order to study the self-association of C5PeC11, solutions of C5PeC11 at different concentrations were titrated into pure xylene, and the experimental data are shown in Figure 2. Injections of C5PeC11 solutions generate negative peaks, indicating that dilution of C5PeC11

solutions is an endothermic process. This process is related to breaking bonds between C5PeC11 molecules due to dissociation of aggregates during the dilution. Figure 2b shows that the heat values obtained by integrating each peak decrease gradually and monotonously with concentrations. This means that the aggregation is progressive with no critical process steps. To obtain the main thermodynamic parameters, a dimer model is used to fit the experimental data as following:

$$(C5PeC11)_2 \leftrightarrow 2(C5PeC11), \{K_{C5PeC11}, \Delta H_{C5PeC11}\} \quad (1)$$

$$K_{C5PeC11} = \frac{[C5PeC11]^2}{[(C5PeC11)_2]} \quad (2)$$

where $K_{C5PeC11}$ is the dissociation constant of the C5PeC11 dimers, $\Delta H_{C5PeC11}$ is the corresponding enthalpy change, [C5PeC11] and [$(C5PeC11)_2$] are the concentration of monomers and dimers, respectively.

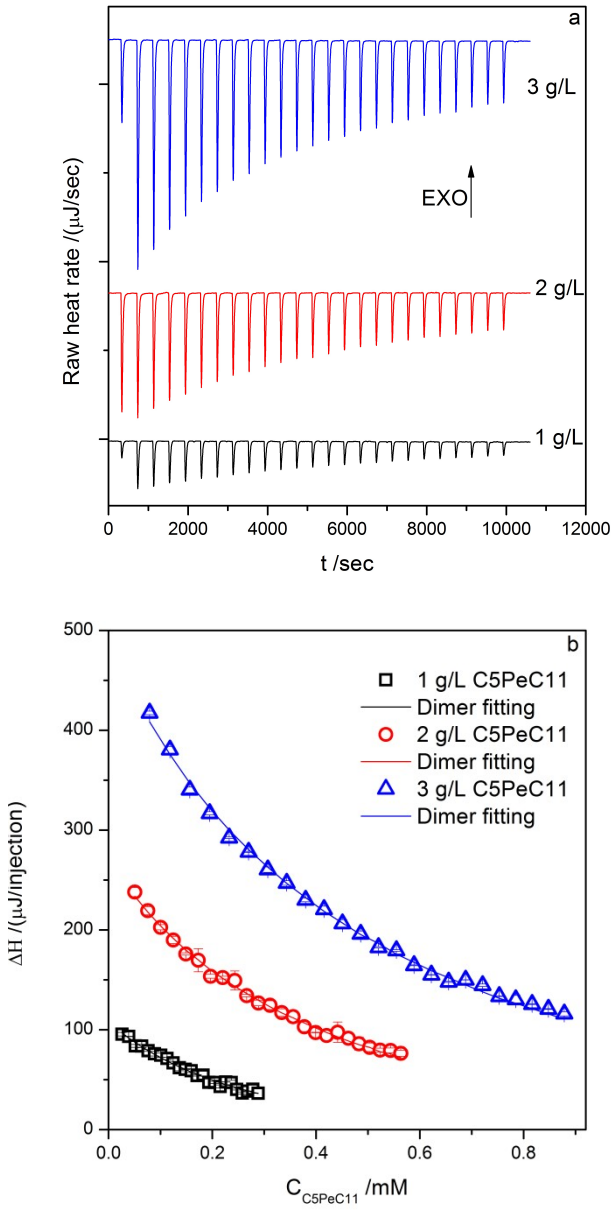

Figure 2. Titration of C5PeC11 at different concentrations in xylene. (a) Experimental data and (b) integrated heats. Lines represent the dimer fitting. The error bar is standard deviation of repeats.

Table 1. Thermodynamic parameters of the dimer dissociation based on curve fitting determined by ITC. The data for extracted asphaltenes are taken from Wei et al. [22]

	Asphaltenes[22]	C5PeC11			BisAC11			Mixture of C5PeC11/ BisAC11 (ratio)	
C (mM)	13.3	1.2	2.4	3.6	9.7	29.0	48.3	9.6(1/3)	14.4(1/5)
K_d (mol/L)	0.01	0.0025	0.0029	0.0032	0.18	0.27	0.40	0.015	0.027
ΔH (kJ/mol)	6.3	44.8	45.9	47.1	10.7	14.8	17.1	15.0	12.6
ΔS (J/mol·K)	58.4	200.0	202.6	205.7	50.1	60.4	64.8	85.5	72.4

It is found that the dimer model perfectly fits the experimental data for all the initial concentrations. The fitted parameters are collected in Table 1. All parameters at different concentrations are consistent, indicating that dimerization is a proper model for the aggregation

level of C5PeC11 in xylene. Both ΔH values and ΔS values are positive. This means that the dimerization process is enthalpy-driven. The enthalpy values for C5PeC11 dimerization are compatible with those of stearic acid (ca. 45 vs ca. 40 kJ/mol).[47] This implies that the hydrogen bonding should be the driving force for the association. The corresponding dissociation constant is almost ten times lower than asphaltenes indicating its higher self-aggregation extent.[46] The dissociation constant allows to calculate the distribution of monomers and dimers which is presented in Figure 3. C5PeC11 mainly exists in a monomeric state at the lowest concentrations (0.1 mM with 94% monomer) and in dimeric state at higher concentrations. The transition between the two regimes happens at a concentration of 2.9 mM at which 50 % of C5PeC11 are present as monomers and the rest as dimers. The results from the fitting of BisAC11 are also shown in Table 1 and Figure 3, which will be discussed in details below.

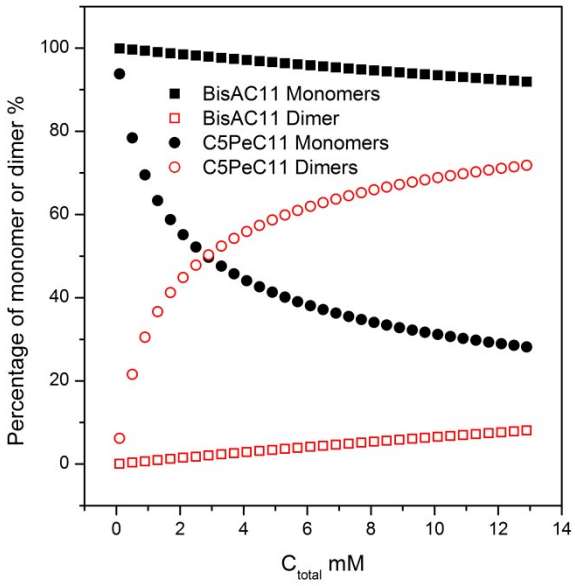

Figure 3. Concentration of monomers and dimers in the cell based on the dissociation constants determined by ITC (Table 1).

Proton NMR spectra are used to detect molecular arrangement of C5PeC11 aggregates. Figure 4 shows the aromatic region of the NMR spectra of C5PeC11 in d-toluene at different concentrations. The resonance peaks for the aromatic protons shift to higher field with increasing C5PeC11 concentration. Interestingly, the resonance peaks corresponding to protons b and c (labels in Figure 4) change from two peaks at 0.1 mM to three peaks at 1.2 mM and even to four peaks at 2.4 mM. These changes are attributed to an evolution of the self-association state of C5PeC11 with the concentration. At lower concentrations (0.1 mM), C5PeC11 mainly exists as

monomers and chemical microenvironment around protons b and c being almost the same, i,e, surrounded by solvent molecules only. This is consistent with ITC results (Figure 3). At higher concentrations (1.2 mM and 2.4 mM), the aggregation becomes more significant, which results in a significant change of the microenvironment around protons b and c. This indicates a dimerization of C5PeC11 in agreement with ITC results. As the self-association process is recorded by protons b and c i.e. aromatic hydrogens, it can be deduced that the aromatic parts of two C5PeC11 molecules stack to each others due to π-π association. Consequently it can be deduced that the dimerization is due to a combination of H-bonds between carboxylic acid groups and π-π association between the polyaromatic rings. Quantitative information can be extracted from the NMR spectra under the following three assumptions:

-C5PeC11 molecules in xylene are assumed to exist mainly in two states, i.e. monomer and dimer.

-The main aggregation state of C5PeC11 at the lowest concentration studied (0.1 mM) is monomer i.e. the chemical shift value ($\delta_{0.1\ mM}$) of the protons is equal to that for monomers ($\delta_{mononer}$).

-The main aggregation state at the highest concentration (2.4 mM) is dimer, the chemical shift value ($\delta_{2.4\ mM}$) is equal to that for dimers (δ_{dimer}).

Consequently,

$$\delta_{obs} = \phi_{\mathrm{dim}er}\delta_{\mathrm{dim}er} + \phi_{monomer}\delta_{monomer} \quad (3)$$

where ϕ_{dimer} is molar fraction of dimers, and $\phi_{monomer}$ of monomers, respectively.

The molar ratio of different species at different concentrations can be estimated based on Eq 3.[48] Hence, the dissociation constants are readily obtained from Eq 2 and summarized in Table 2. It is found that the dissociation constants calculated from different protons are quite consistent at different concentrations even if the dissociation constant decreases when the C5PeC11 concentration increases. This is mostly due to the fact that at 2.4 mM, all the C5PeC11 are not in dimer state (Figure 3) and therefore the 3rd assumption is not completely true. However the most important point is that values reported in Table 2 are similar to the values obtained from the ITC measurements. This verifies the formation of C5PeC11 dimers and the ITC analysis.

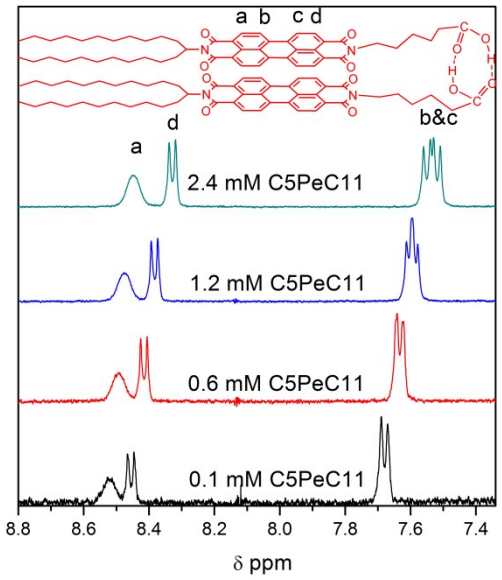

Figure 4. NMR spectra for the protons on aromatic ring of C5PeC11 at different concentrations in d-toluene, and the dimer model.

Table 2. Dissociation constants K_d (mol/L) of C5PeC11 at different concentrations calculated from chemical shift values of different protons.

C	Protons a	Protons b&c	Protons d
0.6 mM	0.0018	0.0012	0.0016
1.2 mM	0.0008	0.0005	0.0007

3.1.2 Self-association of BisAC11

For comparison, the association of BisAC11 is also followed. Figure 5 presents the titration of BisAC11 solutions at different concentrations. Injection of BisAC11 solutions into pure xylene

generates negative peaks indicating endothermic process due to dissociation of BisAC11 aggregates. The enthalpy value generated decreases linearly with concentration. The dimer model is used to fit the experimental data, and the fitted data are listed in Table 1. The experimental data can be well fitted as shown in Figure 5. The obtained parameters (Kd, ΔH and ΔS) present a small increase with BisAC11 concentration. However this trend is small (same order of magnitude for all the concentrations) and could be attributed to uncertainties in the data especially at the lowest BisAC11 concentration. Consequently the dimer model seems to describe correctly the behavior of BisAC11 in bulk. In conclusion, overall these features are similar to the ones reported for C5PeC11 in Table 1. The main difference is that the dissociation enthalpy (ΔH) is much lower than the one corresponding to C5PeC11: The monomers remain predominant within the concentration range studied (up to 13 mM) (Figure 3). BisAC11 shows lower aggregation tendency in xylene due to steric hindrance of the swallow-tail-like side chains and the lack of polar group in the side chains.

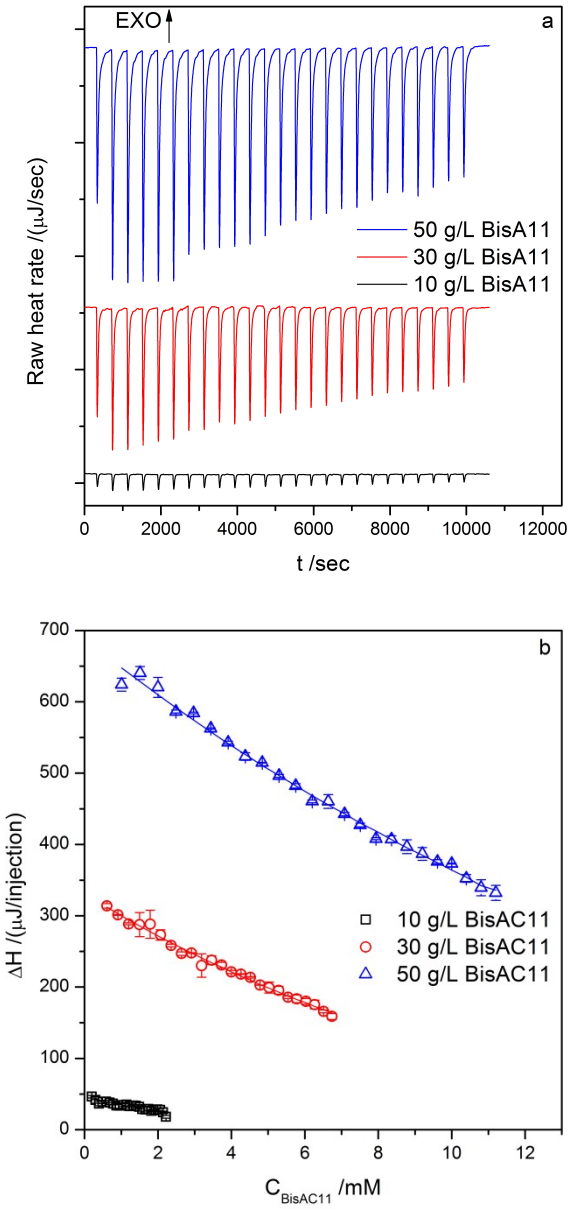

Figure 5. Titration of BisAC11 at different concentrations in xylene: (a) Experimental heat rate and (b) integrated heats.

The self-association properties of BisAC11 have also been studied by NMR (Figure 6). The changes in chemical shifts ($\Delta\delta$ ppm) of the protons on perylene rings of both C5PeC11 and

BisAC11 molecules as a function of concentration are compared in Figure 7. $\Delta\delta$ is obtained by subtraction of observed chemical shift of protons at different concentrations with that of the protons at 0.1 mM. The $\Delta\delta$ value for C5PeC11 exhibits a significant decrease from the initial concentration, whereas the $\Delta\delta$ value for BisAC11 only shows a slight decrease within the same concentration range and a significant decrease is observed until the concentration is up to 9.7 mM (Figures 6 and 7). In conclusion both ITC and NMR results confirm that the main state of BisAC11 is monomeric within the concentration range investigated.

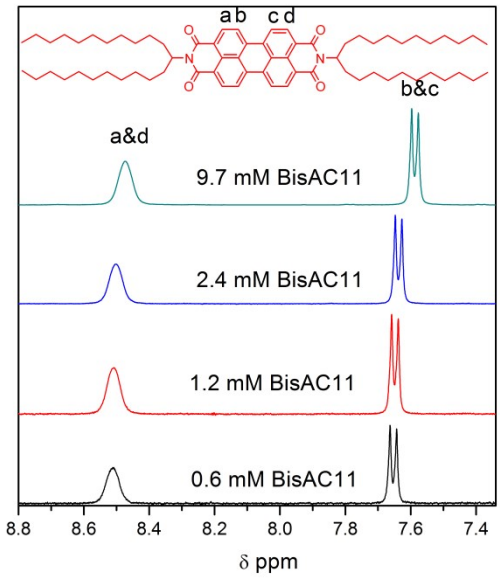

Figure 6. NMR spectra for the protons on aromatic ring of BisAC11 at different concentrations in d-toluene.

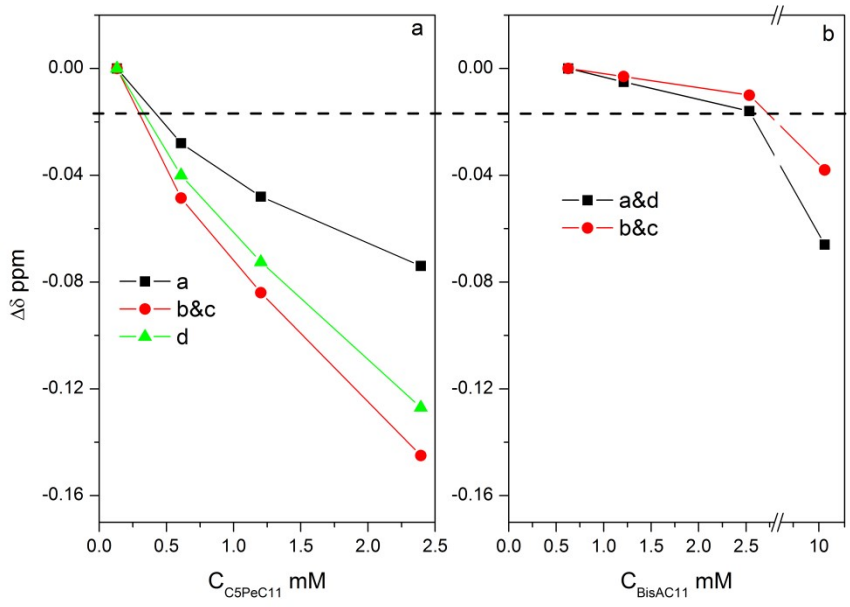

Figure 7. Variation in chemical shift of different protons on the polyaromatic rings of the asphaltene model compounds as a function of concentration: a) C5PeC11; b) BisAC11.

3.1.3 Interactions of different model compounds

In order to mimic the polydisperse asphaltene condition, titrations of mixtures of C5PeC11 and BisAC11 were performed and shown in Figure 8. Two molar ratios of C5PeC11 and BisAC11 (1/3 and 1/5) have been tested (Figures 8 and 9). The enthalpy of the dilutions of mixtures shows the same trends as the dilution process of individual compound solutions. The net values of the enthalpy generated by the dilution of mixtures are slightly higher than those calculated from the data obtained from the dilution of individual compounds taken separately (reported as “Sum of BisAC11 and C5PeC11” in figures 8 and 9). This might be related to specific interactions

between different model compounds. The weak interactions might originate from the π-π stacking of polyaromatic rings of BisAC11 and C5PeC11, which is confirmed by a slight shift of signal of protons b and c in the mixture of BisAC11 and C5PeC11 (Figure 10). The dimer model is also used to fit the experimental data of dilution of the mixtures. The dissociation parameters obtained are close to the values reported for real asphaltenes extracted from crude oil and summarized in Table 1,[46] which implies that the mixtures of the model compounds are able to mimic the self-association behavior of asphaltenes probed by ITC in a quantitative way. This is also consistent with the polydisperse nature of total asphaltene fraction displaying very different association properties.[35] Nevertheless it must be pointed out that the considered model compounds only form dimers while extracted asphaltenes can form higher order aggregates[29, 49], a phenomenon that does not seem to be probed by the ITC technique.

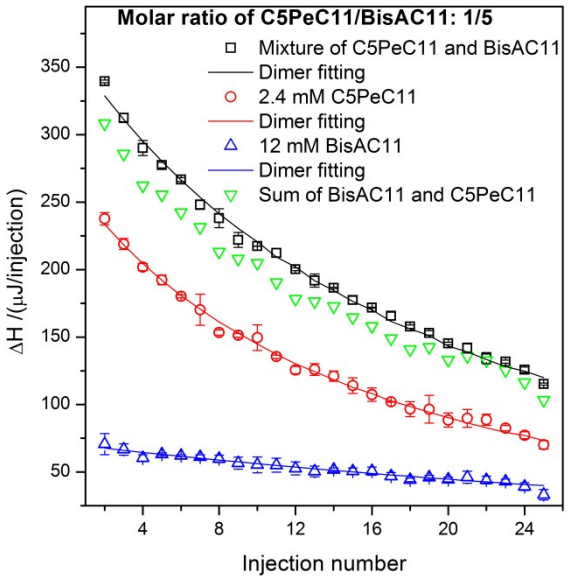

Figure 8. Titrations of individual asphaltene model compound solutions and mixtures of asphaltene model compounds at molar ratio of C5PeC11 and BisAC11 at 1/5.

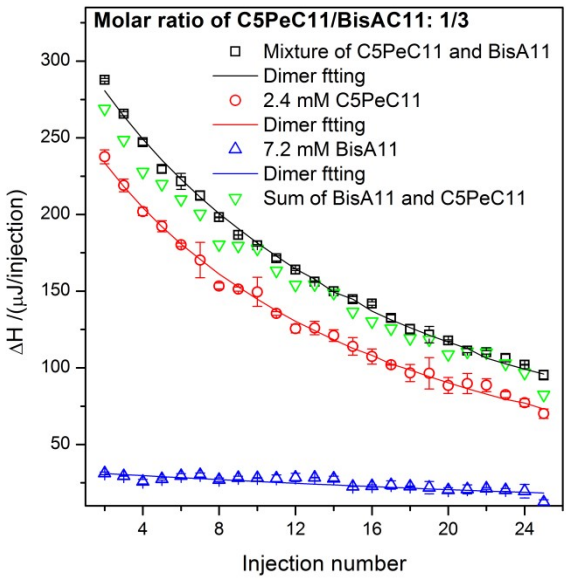

Figure 9. Titrations of individual asphaltene model compound solutions and mixtures of asphaltene model compounds at molar ratio of C5PeC11 and BisAC11 at 1/3.

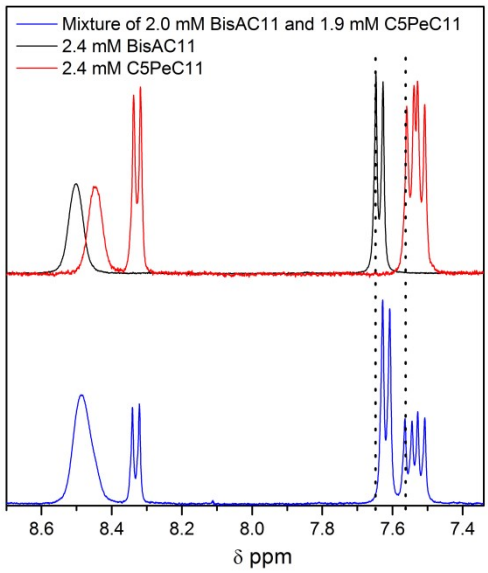

Figure 10. NMR spectra for the protons on aromatic ring for mixture of C5PeC11 and BisAC11 and for individual C5PeC11 and BisAC11 solutions in d-toluene.

3.2 Influence of n-heptane on association and precipitation of C5PeC11

It is well-known that addition of heptane will enhance the aggregation of asphaltenes and eventually lead to their precipitation.[50, 51] For the model compounds, it was also observed that the addition of heptane enhanced significantly the association between C5PeC6 molecules, a molecule similar to C5PeC11 with shorter side alkyl chains.[52] In order to monitor self-association and precipitation processes, the UV-visible spectra of C5PeC11 with increasing heptane content were recorded and displayed in Figure 11. These spectra were measured 4 h after

addition of heptane into C5PeC11 in xylene without filtration. This precipitation can be visually observed after several hours for heptane content higher than 40 vol% (inset, Figure 12). The π HOMO to π* LUMO transition of the model compound monomers is well isolated from other allowed 4-transitions corresponding to ν=0→ν'=0, 1, 2, and 3, where ν and ν' are quantum vibrational numbers of the ground and excited states, respectively.[53] The absorption bands (0-0 at ca. 526 nm) decrease gradually with increasing amount of heptane, while the bands (0-2 and 0-3 at ca. 460 and ca. 432 nm) show a slight increase. The enhancement of bands 0-2 and 0-3 implies strong excitonic interactions between polyaromatic rings.[54] A new band appears at longer wavelength (ca. 560 nm) at 40 vol% heptane, which indicates the formation of crystalline or semi-crystalline precipitates.[54, 55] The absorption values of the crystal band are shown in Figure 12. The absorption values remain the same at low heptane contents, and start to increase abruptly at 40 vol%, and finally approach to a plateau at 70 vol%. To monitor π-π stacking extent,[54] the ratio of intensities of band I_{0-0} and band I_{0-1} is also presented in Figure 12. It is shown that values of the ratios decrease with increasing heptane content, and the inflection point of curves is close to the ones for adsorption band (ca. 560 nm). Decreasing value indicates higher extent of π-π stacking, which might indicate formation of larger aggregates or tighter arrangement of aromatic rings. In conclusion, the variations of the ratio of intensities of band I_{0-0} and band I_{0-1} with heptane content indicates that π- π stacking plays a role in precipitation of

C5PeC11. In the case of BisAC11, the UV-visible spectra remain the same and no crystal band is observed under all conditions studied, which would indicate little variations of the self-association for the compound with the composition of the solvent (Figures 12 and 13).

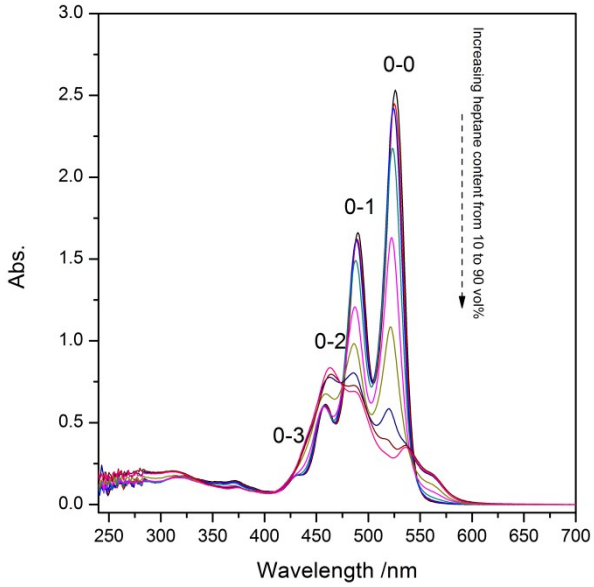

Figure 11. Absorption spectra of 0.2 mM C5PeC11 at different heptane contents from 10 to 90 vol%, the samples were tested after 4 h without filtration.

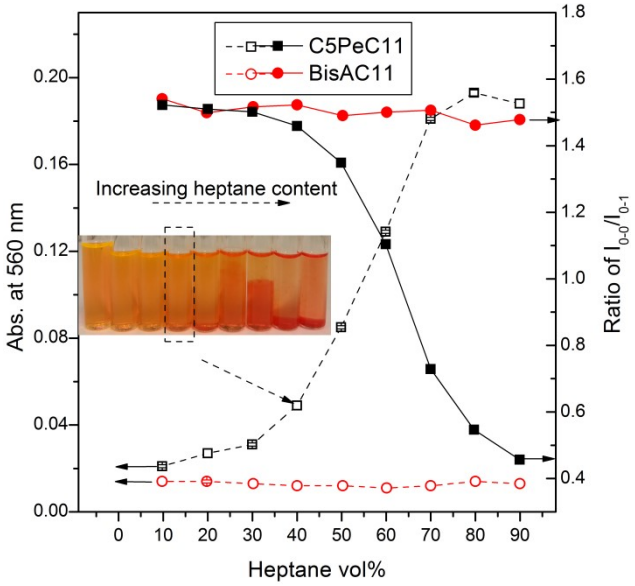

Figure 12. Absorbance value at 560 nm and ratio of $I_{0\text{-}0}/I_{0\text{-}1}$ for 0.2 mM C5PeC11 (squares) and 0.2 mM BisAc11 (circles) as a function of heptane content measured after 4 h; the inset is photographs corresponding to each C5PeC11 samples taken after 24 h. Appearance of a precipate is visible.

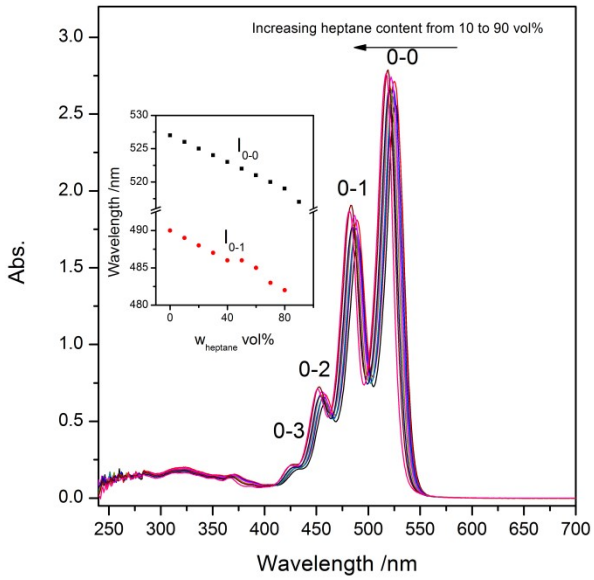

Figure 13. Absorption spectra of 0.2 mM BisAC11 at different heptane contents; the inset represents the wavelength of band 0-0 and 0-1 as a function of heptane content.

4. CONCLUSION

Self-association patterns of different asphaltene model compounds (C5PeC11 and BisAC11) have been investigated. It is found by ITC and NMR that mostly the carboxylic groups make C5PeC11 prone to self-association. Mixtures of different model compounds displaying different self-association patterns can well quantitatively mimic polydisperse asphaltene systems probed by ITC which could imply that asphaltenes are composed of compounds displaying very different association properties. Higher heptane content will promote π-π stacking resulting in precipitation of C5PeC11.

In the second article of the series, the interplay and complexation between model compounds and between model compounds and asphaltene precipitation inhibitors will be studied.

5. CORRESPONDING AUTHOR

*E-mails: sebastien.simon@chemeng.ntnu.no (Sébastien Simon) ; weiduo@yzu.edu.cn (Duo Wei)

**Current address: Testing center, Yangzhou University, Yangzhou, China

6. ACKNOWLEDGEMENTS

The authors thank the JIP Asphaltene consortium “Improved Mechanism of Asphaltene Deposition, Precipitation and Fouling to Minimize Irregularities in Production and Transport (NFR PETROMAKS)”, consisting of Ugelstad Laboratory (NTNU, Norway), University of Alberta (Canada), University of Pau (France), University of Paraná (Brazil) and funded by Norwegian Research Council (234112) and the following industrial sponsors – AkzoNobel, British Petroleum, Canada Natural Resources, Nalco Champion, Petrobras, Statoil and Total E&P Norge AS.

7. REFERENCES

[1] J. Sjoblom, N. Aske, I. Harald Auflem, O. Brandal, T. Erik Havre, O. Saether, A. Westvik, E. Eng Johnsen, H. Kallevik, Our Current Understanding of Water-in-Crude Oil Emulsions.: Recent Characterization Techniques and High Pressure Performance, Adv. Colloid Interface Sci., 100-102 (2003) 399-473.

[2] J.G. Speight, Petroleum asphaltenes - Part 1: Asphaltenes, resins and the structure of petroleum Oil & Gas Sci. Technol., 59 (2004) 467-477

[3] J.G. Speight, The Chemistry and Technology of Petroleum, 4th Edition, CRC Press, 2007.

[4] J. Sjöblom, S. Simon, Z. Xu, Model molecules mimicking asphaltenes, Adv. Colloid Interface Sci., 218 (2015) 1-16.

[5] J.D. McLean, P.K. Kilpatrick, Effects of Asphaltene Aggregation in Model Heptane-Toluene Mixtures on Stability of Water-in-Oil Emulsions, J. Colloid Interface Sci., 196 (1997) 23-34.

[6] J.D. McLean, P.K. Kilpatrick, Effects of Asphaltene Solvency on Stability of Water-in-Crude-Oil Emulsions, J. Colloid Interface Sci., 189 (1997) 242-253.

[7] Y.H. Shokrlu, R. Kharrat, M.H. Ghazanfari, S. Saraji, Modified screening criteria of potential asphaltene precipitation in oil reservoirs, Petrol. Sci. Technol., 29 (2011) 1407-1418.

[8] W. Kleinitz, S.I. Andersen, Asphaltene precipitates in oil production wells, Oil Gas Eur. Mag., 24 (1998) 30-33.

[9] R. Thawer, D.C.A. Nicoll, G. Dick, Asphaltene Deposition in Production Facilities, SPE Prod. Eng., (1990) 475-480.

[10] M. Deo, M. Parra, Characterization of carbon-dioxide-induced asphaltene precipitation, Energy Fuels, 26 (2012) 2672-2679.

[11] I.A. Wiehe, R.J. Kennedy, The oil compatibility model and crude oil incompatibility, Energy Fuels, 14 (1999) 56-59.

[12] L. Buch, H. Groenzin, E. Buenrostro-Gonzalez, S.I. Andersen, C. Lira-Galeana, O.C. Mullins, Molecular size of asphaltene fractions obtained from residuum hydrotreatment, Fuel, 82 (2003) 1075-1084.

[13] H. Groenzin, O.C. Mullins, Asphaltene Molecular Size and Structure, J. Phys. Chem. A, 103 (1999) 11237-11245.

[14] H. Groenzin, O.C. Mullins, Molecular size and structure of asphaltenes from various sources, Energy Fuels, 14 (2000) 677-684.

[15] H. Groenzin, O.C. Mullins, Molecular size and structure of asphaltenes, Petrol. Sci. Technol., 19 (2001) 219-230.

[16] H. Groenzin, O.C. Mullins, S. Eser, J. Mathews, M.G. Yang, D. Jones, Molecular Size of Asphaltene Solubility Fractions, Energy Fuels, 17 (2003) 498-503.

[17] A.R. Hortal, B. Martínez-Haya, M.D. Lobato, J.M. Pedrosa, S. Lago, On the determination of molecular weight distributions of asphaltenes and their aggregates in laser desorption ionization experiments, J. Mass Spectrom., 41 (2006) 960-968.

[18] A.E. Pomerantz, M.R. Hammond, A.L. Morrow, O.C. Mullins, R.N. Zare, Two-step laser mass spectrometry of asphaltenes, J. Am. Chem. Soc., 130 (2008) 7216-7217.

[19] J. Murgich, Molecular simulation and the aggregation of the heavy fractions in crude oils, Mol. Simulat., 29 (2003) 451-461.

[20] O.C. Mullins, The modified Yen model, Energy Fuels, 24 (2010) 2179-2207.

[21] N. Hosseinpour, A.A. Khodadadi, A. Bahramian, Y. Mortazavi, Asphaltene Adsorption onto Acidic/Basic Metal Oxide Nanoparticles toward in Situ Upgrading of Reservoir Oils by Nanotechnology, Langmuir, 29 (2013) 14135-14146.

[22] J. Peng, G.Q. Tang, A.R. Kovscek, Oil chemistry and its impact on heavy oil solution gas drive, Journal of Petroleum Science and Engineering, 66 (2009) 47-59.

[23] M.A. Anisimov, I.K. Yudin, V. Nikitin, G. Nikolaenko, A. Chernoutsan, H. Toulhoat, D. Frot, Y. Briolant, Asphaltene aggregation in hydrocarbon solutions studied by photon correlation spectroscopy, J. Phys. Chem, 99 (1995) 9576-9580.

[24] I.K. Yudin, G.L. Nikolaenko, E.E. Gorodetskii, E.L. Markhashov, V.A. Agayan, M.A. Anisimov, J.V. Sengers, Crossover kinetics of asphaltene aggregation in hydrocarbon solutions, Physica A, 251 (1998) 235-244.

[25] D. Merino-Garcia, J. Murgich, S.I. Andersen, Asphaltene self-association: modeling and effect of fractionation with a polar solvent, Petrol. Sci. Technol., 22 (2004) 735-758.

[26] M. Fossen, H. Kallevik, K.D. Knudsen, J. Sjöblom, Asphaltenes precipitated by a two-step precipitation procedure. 1. Interfacial tension and solvent properties, Energy Fuels, 21 (2007) 1030-1037.

[27] J.A. Ostlund, M. Nyden, H.S. Fogler, K. Holmberg, Functional groups in fractionated asphaltenes and the adsorption of amphiphilic molecules, Colloid Surf. A, 234 (2004) 95-102.

[28] P.M. Spiecker, K.L. Gawrys, P.K. Kilpatrick, Aggregation and solubility behavior of asphaltenes and their subfractions, J. Colloid Interface Sci., 267 (2003) 178-193.

[29] L. Barre, S. Simon, T. Palermo, Solution Properties of Asphaltenes, Langmuir, 24 (2008) 3709-3717.

[30] D. Fenistein, L. Barre, Experimental measurement of the mass distribution of petroleum asphaltene aggregates using ultracentrifugation and small-angle X-ray scattering, Fuel, 80 (2001) 283-287.

[31] J. Marques, D. Guillaume, I. Merdrignac, D. Espinat, L. Barré, S. Brunet, Ultrafiltration des asphaltènes par filtration tangentielle et méthodologie de reconstitution des charges, Oil & Gas Sci. Technol. - Rev. IFP, 64 (2009) 795-806.

[32] J. Marques, I. Merdrignac, A. Baudot, L. Barré, D. Guillaume, D. Espinat, S. Brunet, Séparation des asphaltènes par nano et ultrafiltration – Comparaison avec la méthode de floculation, Oil & Gas Sci. Technol. - Rev. IFP, 63 (2008) 139-149.

[33] K. Akbarzadeh, D.C. Bressler, J. Wang, K.L. Gawrys, M.R. Gray, P.K. Kilpatrick, H.W. Yarranton, Association behavior of pyrene compounds as models for asphaltenes, Energy Fuels, 19 (2005) 1268-1271.

[34] F. Rakotondradany, H. Fenniri, P. Rahimi, K.L. Gawrys, P.K. Kilpatrick, M.R. Gray, Hexabenzocoronene model compounds for asphaltene fractions: synthesis & characterization, Energy Fuels, 20 (2006) 2439-2447.

[35] E.L. Nordgård, E. Landsem, J. Sjöblom, Langmuir Films of Asphaltene Model Compounds and Their Fluorescent Properties, Langmuir, 24 (2008) 8742-8751.

[36] T. Kuznicki, J.H. Masliyah, S. Bhattacharjee, Aggregation and partitioning of model asphaltenes at toluene−water interfaces: molecular dynamics simulations, Energy Fuels, 23 (2009) 5027-5035.

[37] E.L. Nordgård, J. Sjöblom, Model Compounds for Asphaltenes and C80 Isoprenoid Tetraacids. Part I: Synthesis and Interfacial Activities, J. Dispersion Sci. Technol., 29 (2008) 1114 - 1122.

[38] E.L. Nordgård, G. Sørland, J. Sjöblom, Behavior of Asphaltene Model Compounds at W/O Interfaces, Langmuir, 26 (2009) 2352-2360.

[39] A.L. Nenningsland, B. Gao, S. Simon, J. Sjöblom, Comparative study of stabilizing agents for water-in-oil emulsions, Energy Fuels, 25 (2011) 5746-5754.

[40] M.R. Gray, R.R. Tykwinski, J.M. Stryker, X. Tan, Supramolecular assembly model for aggregation of petroleum asphaltenes, Energy Fuels, 25 (2011) 3125-3134.

[41] M. Sedghi, L. Goual, W. Welch, J. Kubelka, Effect of asphaltene structure on association and aggregation using molecular dynamics, J. Phys. Chem. B, 117 (2013) 5765-5776.

[42] C. Jian, T. Tang, S. Bhattacharjee, Probing the effect of side-chain length on the aggregation of a model asphaltene using molecular dynamics simulations, Energy Fuels, 27 (2013) 2057-2067.

[43] F. López-Linares, L. Carbognani, M.F. González, C. Sosa-Stull, M. Figueras, P. Pereira-Almao, Quinolin-65 and violanthrone-79 as model molecules for the kinetics of the adsorption of C7 athabasca asphaltene on macroporous solid surfaces, Energy Fuels, 20 (2006) 2748-2750.

[44] O.C. Mullins, H. Sabbah, J. Eyssautier, A.E. Pomerantz, L. Barre, A.B. Andrews, Y. Ruiz-Morales, F. Mostowfi, R. McFarlane, L. Goual, R. Lepkowicz, T. Cooper, J. Orbulescu, R.M. Leblanc, J. Edwards, R.N. Zare, Advances in asphaltene science and the Yen-Mullins model, Energy Fuels, 26 (2012) 3986-4003.

[45] M.W. Holman, R. Liu, D.M. Adams, Single-molecule spectroscopy of interfacial electron transfer, J. Am. Chem. Soc., 125 (2003) 12649-12654.

[46] D. Wei, E. Orlandi, S. Simon, J. Sjöblom, M. Suurkuusk, Interactions between asphaltenes and alkylbenzene-derived inhibitors investigated by isothermal titration calorimetry, J. Therm. Anal. Calorim., 120 (2015) 1835-1846.

[47] D. Wei, E. Orlandi, M. Barriet, S. Simon, J. Sjoblom, Aggregation of tetrameric acid in xylene and its interaction with asphaltenes by isothermal titration calorimetry, J. Therm. Anal. Calorim., (2015).

[48] O. Söderman, P. Guering, On the determination of micellar aggregation numbers from the concentration dependence of13C NMR chemical shifts, Colloid & Polymer Sci, 265 (1987) 76-82.

[49] D. Fenistein, L. Barre, D. Broseta, D. Espinat, A. Livet, J.N. Roux, M. Scarsella, Viscosimetric and Neutron Scattering Study of Asphaltene Aggregates in Mixed Toluene/Heptane Solvents, Langmuir, 14 (1998) 1013-1020.

[50] I.K. Yudin, G.L. Nikolaenko, E.E. Gorodetskii, V.I. Kosov, V.R. Melikyan, E.L. Markhashov, D. Frot, Y. Briolant, Mechanisms of asphaltene aggregation in toluene–heptane mixtures, J. Petrol. Sci. Eng., 20 (1998) 297-301.

[51] D. Merino-Garcia, S.I. Andersen, Application of isothermal titration calorimetry in the *i*nvestigation of asphaltene association, in: O. Mullins, E. Sheu, A. Hammami, A. Marshall (Eds.) Asphaltenes, Heavy Oils, and Petroleomics, Springer New York, 2007, pp. 329-352.

[52] J. Wang, N. van der Tuuk Opedal, Q. Lu, Z. Xu, H. Zeng, J. Sjöblom, Probing molecular interactions of an asphaltene model compound in organic solvents using a surface forces apparatus (SFA), Energy Fuels, 26 (2011) 2591-2599.

[53] W. Wang, J.J. Han, L.Q. Wang, L.S. Li, W.J. Shaw, A.D.Q. Li, Dynamic π–π stacked molecular assemblies emit from green to red colors, Nano Lett., 3 (2003) 455-458.

[54] K. Balakrishnan, A. Datar, R. Oitker, H. Chen, J. Zuo, L. Zang, Nanobelt self-assembly from an organic n-type semiconductor: propoxyethyl-PTCDI, J. Am. Chem. Soc., 127 (2005) 10496-10497.

[55] R. van der Weegen, P.A. Korevaar, P. Voudouris, I.K. Voets, T.F.A. de Greef, J.A.J.M. Vekemans, E.W. Meijer, Small sized perylene-bisimide assemblies controlled by both cooperative and anti-cooperative assembly processes, Chem. Commun., 49 (2013) 5532-5534.

1

2